analytical chemistry

Letter

Cite This: *Anal. Chem.* XXXX, XXX, XXX−XXX

pubs.acs.org/ac

High Spatial Resolution Imaging Mass Spectrometry Reveals Chemical Heterogeneity Across Bacterial Microcolonies

Rita de Cassia Pessotti, Bridget L. Hansen, Vineetha M. Zacharia, Daniel Polyakov, and Matthew F. Traxler*

University of California, Berkeley, 111 Koshland Hall, Berkeley, California 94720, United States

Supporting Information

ABSTRACT: Microbes interact with the world around them at the chemical level. However, directly examining the chemical exchange between microbes and microbes and their environment, at ecological scales, i.e., the scale of a single bacterial cell or small groups of cells, remains a key challenge. Here we address this obstacle by presenting a methodology that enables matrix-assisted laser desorption/ionization (MALDI) imaging mass spectrometry (IMS) of bacterial microcolonies. By combining optimized sample preparation with subatmospheric pressure MALDI, we demonstrate that chemical output from groups of as few as ∼50 cells can be visualized with MALDI-IMS. Application of this methodology to *Bacillus subtilis* and *Streptomyces coelicolor* revealed heterogeneity in chemical output across microcolonies and asymmetrical metabolite production when cells grew within physiological gradients produced by *Medicago sativa* roots. Taken together, these results indicate that MALDI-IMS can readily visualize metabolites made by very small assemblages of bacterial cells and that even these small groups of cells can differentially produce metabolites in response to local chemical gradients.

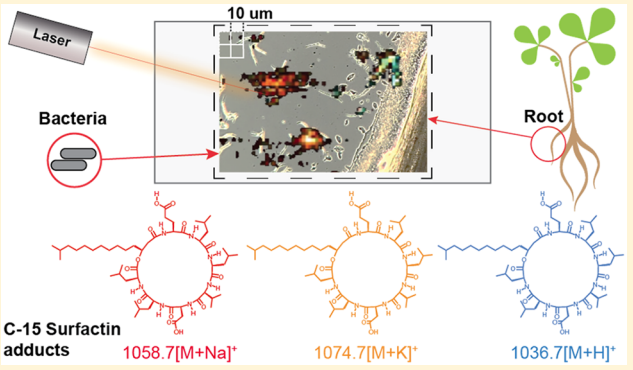

Microbes modify their local chemical environments in multiple ways, including by depleting nutrients, excreting metabolic waste, and producing public goods such as siderophores and biofilm matrixes.[1−3] Many microbes also make a wide array of specialized metabolites, which are thought to mediate interactions ranging from chemical warfare to cooperative coordination.[4,5] Additionally, bacteria may modify the lipid content of their membranes depending on environmental conditions.[6−8] Gaining an understanding of how microbes respond to, and alter, their local chemical environments *in situ* will require methodologies that provide spatial information about microbial chemistry at micrometer scales. Such methodologies will be critical for understanding the chemical exchange that occurs between microbes in the context of microbiomes.

Matrix-assisted laser desorption/ionization (MALDI) imaging mass spectrometry (IMS) is a promising technique for assessing spatial patterns of microbial chemistry.[9−11] To this point, direct MALDI-IMS of microbes has mostly been applied to macroscale colonies. These structures are relatively large (e.g., millimeters in diameter), and spatial resolutions of ∼400−600 μm pixels have been sufficient to visualize differential metabolite production.[9−11] However, the limits of MALDI-IMS remain to be explored in terms of visualizing molecules produced by bacteria at ecologically relevant spatial scales, i.e., on the order of 1−100 μm. Here we describe a methodology for microbial sample preparation and analysis using subatmospheric pressure MALDI-IMS to visualize metabolites produced by microcolonies of bacteria with high spatial resolution. Using this methodology, we find that very small assemblages of bacterial cells show a surprisingly high degree of chemical heterogeneity at microscopic scales.

EXPERIMENTAL SECTION

Strains and Growth Conditions. *Bacillus subtilis* 3610 and *Streptomyces coelicolor* M145 were grown separately on top of agarose pads mounted on ITO-coated microscope slides and incubated at room temperature (RT) for 14 h and 2 days, respectively (see the Supporting Information for more details). For root-bacteria interaction experiments, *B. subtilis* and *S. coelicolor* were inoculated on agarose pads mounted on ITO-coated microscope slides as described above. One-week old sterile *Medicago sativa* roots were laid across the top of each agarose pad and incubated at RT for 14 h for *B. subtilis* or at 30 °C for 4 days for *S. coelicolor*. Negative controls containing only roots atop sterile agarose pads were incubated for 14 h at RT.

Sample Preparation for MALDI-IMS and MALDI-MS/MS. Samples were dried in an incubator at 65 °C for 30 min. A mix of calibration standards (MSCal4, Sigma-Aldrich) was

Received: August 26, 2019
Accepted: November 7, 2019
Published: November 7, 2019

DOI: 10.1021/acs.analchem.9b03909
Anal. Chem. XXXX, XXX, XXX−XXX

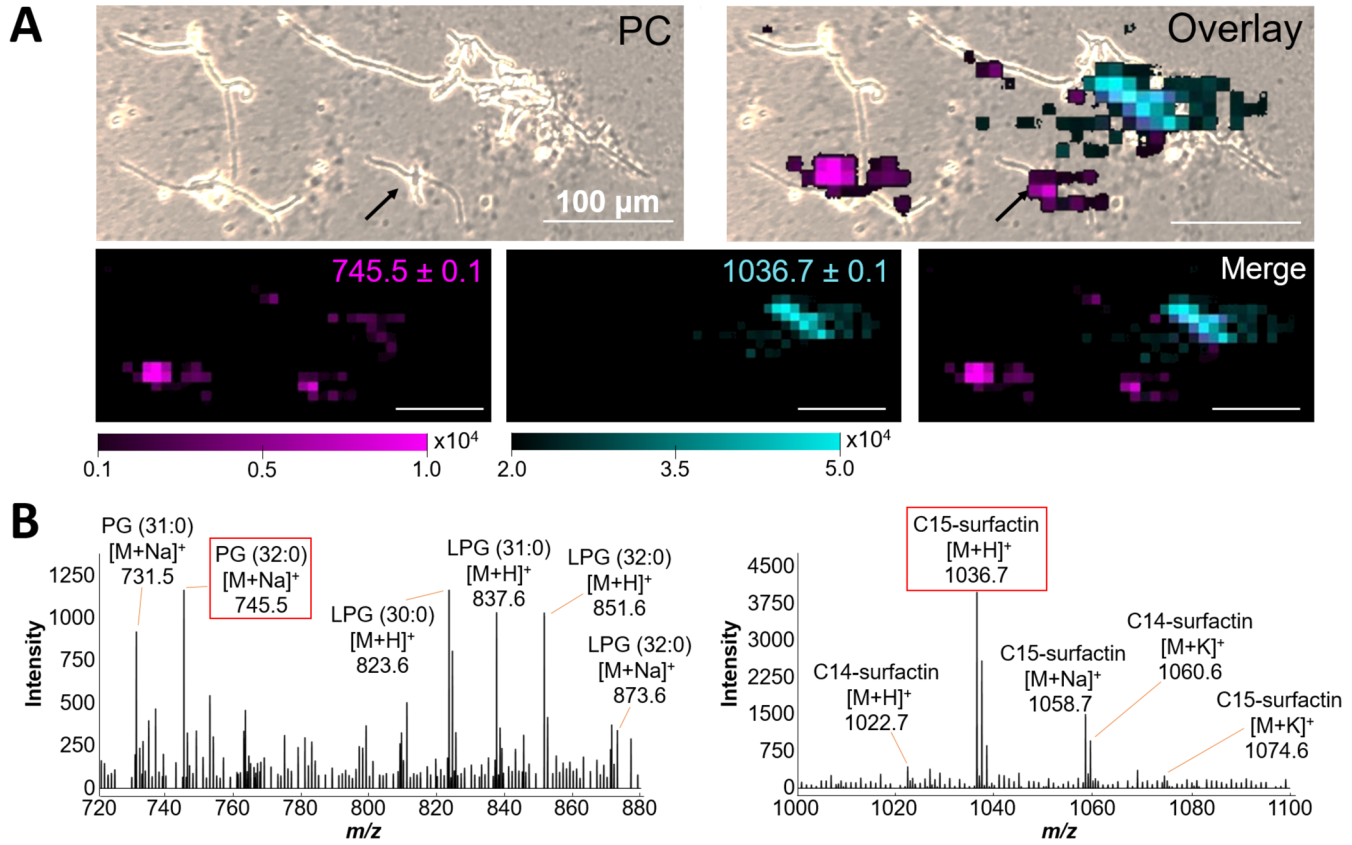

Figure 1. Features associated with*B. subtilis*microcolonies are detectable at micron scales by MALDI-IMS. (A) Micrograph of *B. subtilis* microcolonies and MALDI images showing the spatial distribution of two of the detected features: m/z 745.5 ± 0.1 [sodium adduct of the lipid PG (32:0)] and m/z 1036.7 ± 0.1 (proton adduct of C15-surfactin). Scale bar = 100 μm. The black arrow points to a microcolony that measures ∼120 μm. Micrograph was acquired using a phase contrast (PC) microscope. (B) Corresponding MS1 spectra of the lipids and surfactins detected from *B. subtilis* microcolonies. These average MS1 spectra were acquired from regions of the image where the corresponding ions were seen at high local abundance. MS1 spectra including the full m/z range are shown in Fig. S7.

spotted on each microscope slide to assess signal intensity and mass accuracy for each sample analyzed. Phase contrast images were acquired using an inverted microscope (Zeiss Primovert) equipped with phase contrast objectives (100×, 200×, and 400× magnification) and areas of interest framed by hand with a fine-tip lab marker. MALDI matrix was applied to the samples as described in ref 12 with minor modifications. Briefly, the matrix Super-DHB (Sigma-Aldrich) was sublimated under vacuum (0.05 Torr) for 5 min, with a temperature starting at 30 °C and ending at 95 °C, leading to a matrix deposition of ∼0.25−0.5 mg/cm^2. Samples were not rehydrated post matrix deposition.

MALDI-IMS and MALDI-MS/MS. MALDI-IMS was performed in positive ion mode using a SubAP/MALDI(ng) source (MassTech, Columbia, MD). This ionization source has a small laser spot size (<10 μm) which provides high spatial resolution and is equipped with an ion funnel, which focuses ions into the mass spectrometer, improving the signal-to-noise ratio.[13] This SubAP/MALDI(ng) source was coupled to a Thermo Q-Exactive (Thermo Fisher Scientific, San Jose, CA) high-resolution mass spectrometer. Full MS1 scans were acquired in positive mode, with mass ranges of m/z 100−2000, with a typical range of 600−1600 (see the Supporting Information for more details). The laser energy was 50−80% at 1 kHz repetition rate. Images were acquired using a pixel size of 10 μm at a laser velocity of 1.5 mm/min. Images were analyzed and processed using Datacube Explorer v2.3,[14] MSiReader v1.01,[15] and ImageJ v1.52a.[16] Signal intensities were adjusted to allow clear visualization.

Compound Identification. Compounds were identified at multiple confidence levels according to the scheme proposed by Schymanski et al.[17] These results are summarized for each ID in Tables S1 and S2.

RESULTS AND DISCUSSION

IMS of Bacterial Microcolonies. To determine if features from microcolonies of bacteria could be detected by MALDI-IMS, we inoculated the well-characterized organisms *Bacillus subtilis* 3610 and *Streptomyces coelicolor* M145 directly onto thin pads of agarose mounted on indium-tin oxide (ITO) coated microscope slides. These microbes were selected because they produce several well-characterized families of specialized metabolites and membrane lipids under standard laboratory conditions. Strains were inoculated onto agarose pads in 15 μL volumes of 25% strength ISP2 medium and incubated for 14 h (*B. subtilis*) or 48 h (*S. coelicolor*). This allowed growth of individual *B. subtilis* cells into microcolonies of cell chains in the range of 100−200 μm long and microcolonies of *S. coelicolor* in the range of 100−300 μm in diameter. Micrographs of the colonies were acquired using a phase contrast microscope, the samples were dried, and MALDI matrix was sublimated onto the surface of the sample to achieve a uniform layer of fine matrix crystals. The sample was then imaged with a pixel size of 10 μm using a

DOI: 10.1021/acs.analchem.9b03909
Anal. Chem. XXXX, XXX, XXX−XXX

subatmospheric pressure MALDI source equipped with an ion funnel[13] coupled to an Orbitrap Q-Exactive mass spectrometer, a combination that provides both high spatial and high mass resolution.

Analysis of the MALDI images revealed a variety of chemical features with spatial distributions that matched the cellular arrangement seen in the phase contrast micrographs with surprising fidelity (Figures 1A and 2A, Figs. S2 and 3). We

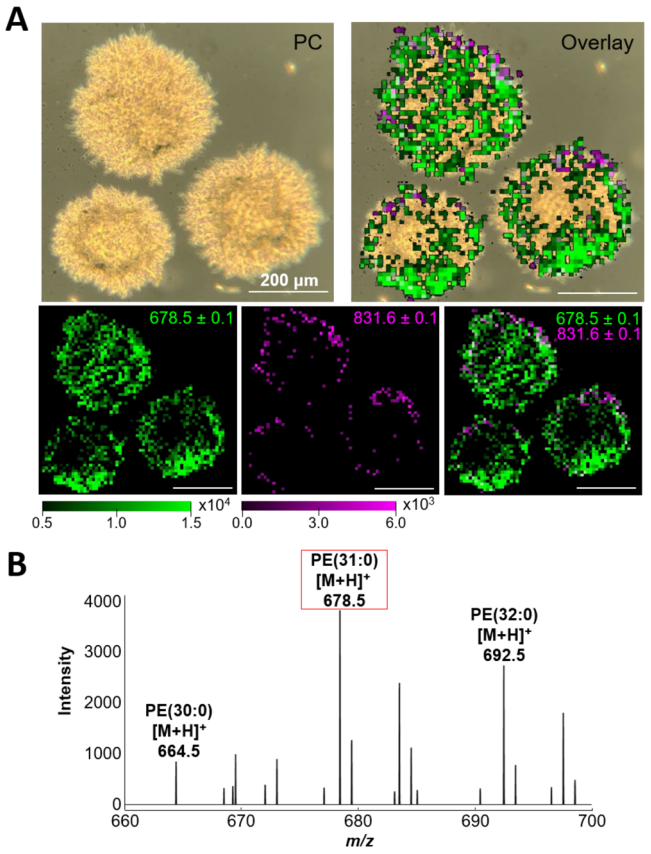

Figure 2. Features associated with *S. coelicolor* microcolonies are detectable at micron scales by MALDI-IMS. (A) Micrograph of *S. coelicolor* microcolonies and MALDI images showing the spatial distribution of two detected features: m/z 678.4 ± 0.1 [putative proton adduct of the lipid PE(31:0)] and m/z 831.6 ± 0.1 (a putative uncharacterized lipid). Scale bar = 200 μm. Micrograph was acquired using a phase contrast (PC) microscope. (B) Corresponding MS1 spectra of the lipids detected from *S. coelicolor* microcolonies. MS1 spectra including the full m/z range, are shown in Fig. S7.

were able to chemically identify a subset of the features (Figures 1B and 2B, Tables S1 and S2) based on exact mass and MS/MS fragmentation patterns. While the absolute intensities of many of these chemical features were relatively low, the robust signal-to-noise ratio provided by this methodology (Fig. S7) enabled high-confidence identifications.

For *B. subtilis* identified features included the lipopeptide specialized metabolite C15-surfactin $[M + H]^+$ (m/z 1036.7) (Figs. S1 and S3) and multiple species of membrane lipids, exemplified by the phosphotidylglycerol (PG) (32:0) $[M + Na]^+$ (m/z 745.5) (Figs. S1 and S3). The MS/MS fragmentation pattern of the ion with the m/z 1036.7, detected in a sample of *B. subtilis* macrocolony, was identical to that of an authentic commercial standard (Fig. S3). Under these conditions, surfactin was only detectable in the largest microcolonies, while membrane lipids were detectable in almost all microcolonies (Figure 1A, Fig. S2). Given the known size range for *B. subtilis* cells,[18] we calculate that the colony marked with a black arrow in Figure 1A is comprised of 26−52 cells.

For *S. coelicolor*, we detected multiple features that correlate with phosphatidylethanolamine (PE) lipids (e.g., m/z 678.5, Figure 2B)[7] and a separate series of features previously hypothesized to represent a set of uncharacterized lipids exemplified by m/z 831.6[19] (Figure 2A, Figs. S4 and S6). Interestingly, the PE lipids were distributed across the entirety of the microcolonies, while the uncharacterized lipids were localized to the outer periphery of the colonies (Figure 2A, Fig. S5). These observations are consistent with the dynamic lipidome made by this organism.[7] Together, these results demonstrate that metabolites produced by bacterial microcolonies comprised of relatively low numbers of cells can be readily detected using MALDI-IMS.

IMS of Bacterial Microcolonies in Physiological Microgradients. The methodology presented here could provide insight into the chemical responses of microbes to physiological microgradients, such as those that likely occur in natural environments. Therefore, we sought to image microcolonies growing in the context of a naturally produced nutrient gradient. To do so, we inoculated *B. subtilis* and *S. coelicolor* onto slide-mounted agarose pads and laid living *M. sativa* roots across them. This setup led to bacterial microcolonies which grew at varying distances from the root and hence experienced a differential gradient of nutrients available in root exudates.

MALDI-IMS revealed asymmetric production of metabolites across and within bacterial microcolonies within this nutrient gradient. For example, the $[M + H]^+$ adduct of surfactin was seen in microcolonies of *B. subtilis* nearest the root after 14 h of growth, while specific membrane lipids were detectable in microcolonies farther away from the root (Figure 3A, Figs. S1 and S2). Control samples that contained roots but were not inoculated with bacteria did not show these chemical features (Figs. S8−S11). These findings are consistent with the proposed role of surfactin in initiating biofilm formation on plant roots,[20−22] although this has never been observed at the chemical level at the microcolony scale. This observation is also in broad agreement with the findings of Debois and coworkers, who saw surfactin produced by *Bacillus amyloliquefaciens* biofilms on tomato and *Arabidopsis* roots after 24 h of colonization using IMS at a macroscale.[23] We also observed that the different surfactin adducts $[M + H]^+$, $[M + Na]^+$, and $[M + K]^+$ showed subtly distinct distributions (Figure 3B), a phenomenon that was also observed by Debois et al.[22,23] at the macroscale, indicating that the root likely generated a microgradient of cations. Thus, the methodology presented here can shed light on the spatial distribution of the chemistry involved in the very early stages of root colonization, when metabolite biosynthesis is heterogeneous at the level of individual microcolonies.

The lipidome of *S. coelicolor* is complex and dynamic.[7] Interestingly, an asymmetrical distribution of multiple lipid-associated features was observed within a single *S. coelicolor* microcolony grown in proximity to the root (Figure 4). An exemplary feature with m/z of 831.6 was only detected on the side of the colony facing away from the root. Other members of this putative lipid class showed a similar localization (Fig. S5). This distribution is in contrast to other colony-associated

DOI: 10.1021/acs.analchem.9b03909
Anal. Chem. XXXX, XXX, XXX−XXX

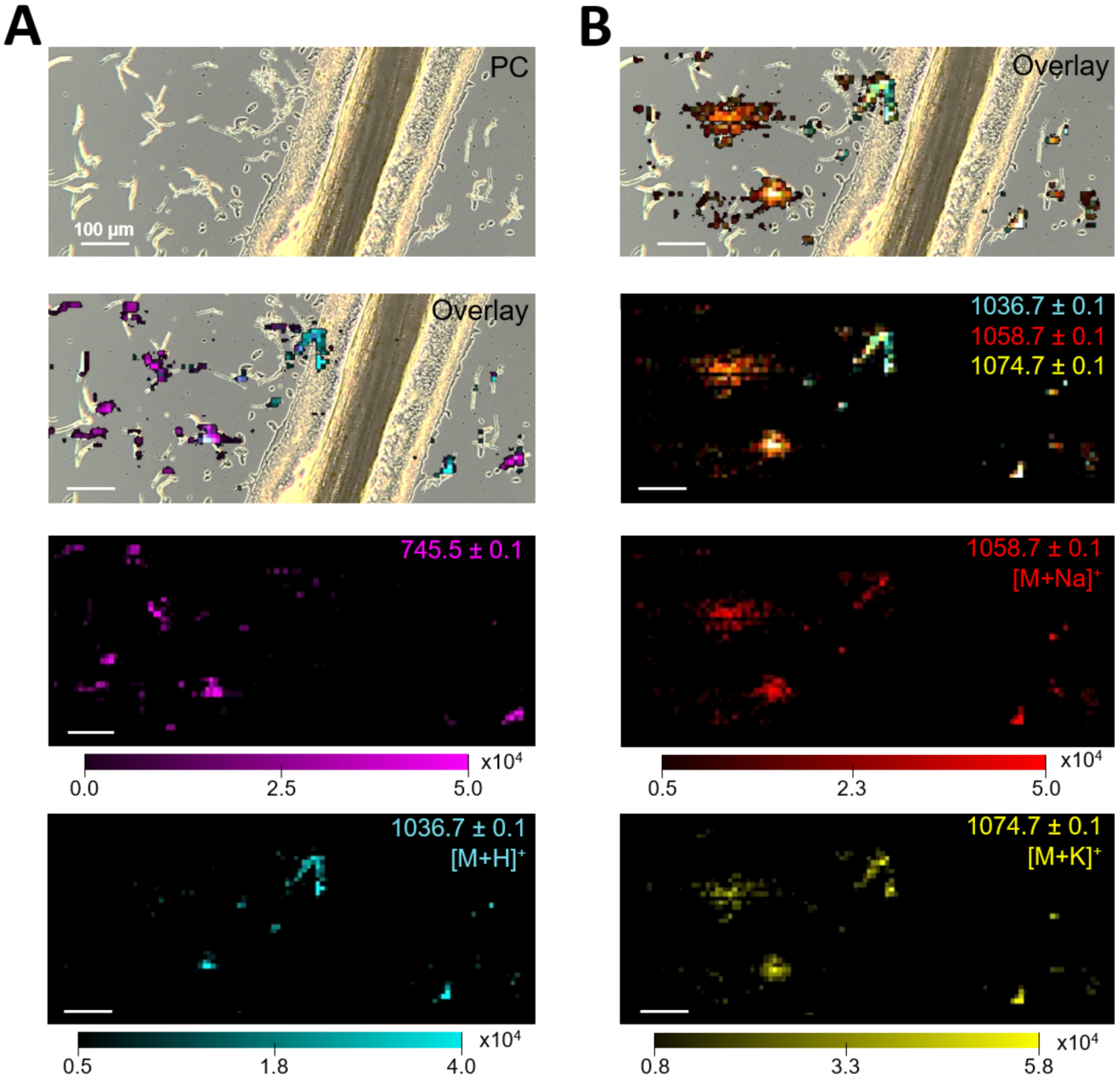

Figure 3. *B. subtilis* microcolonies display asymmetrical ion distribution when grown in proximity to *M. sativa* roots. (A) Micrograph of *B. subtilis* microcolonies growing near a *M. sativa* root; MALDI images show the spatial distribution of two of the detected features: m/z 745.5 ± 0.1 [sodium adduct of the lipid PG (32:0)] and m/z 1036.7 ± 0.1 (proton adduct of C15-surfactin). Note that surfactin was detected in microcolonies nearest the root. The micrograph was acquired using a phase contrast (PC) microscope. (B) MALDI images of surfactin adducts (H^+, Na^+, and K^+) show different spatial distributions.

features that were localized to the side of the colony facing the root (e.g., m/z 845.9). *S. coelicolor* membrane lipid composition has been shown to vary depending on nutrient availability, pH, and osmolarity.[7] Thus, the spatially variable lipid profile we observe here likely reflects a tailored response to these types of microgradients produced by the root. This example illustrates the utility of high spatial resolution MALDI-IMS for exploring differential production of cellular components within single bacterial microcolonies.

CONCLUSION

The results presented here demonstrate the feasibility of using MALDI-IMS for visualizing microbial chemistry at ecologically relevant spatial scales. This advance reflects improvements in sample preparation and ionization via subatmospheric MALDI coupled with an ion funnel, which we report in detail in the Supporting Information. This methodology enables the visualization of metabolites differentially produced by individual microbial microcolonies composed of as few as ~50 cells.

Using this methodology, we found that even small assemblages of bacterial cells can produce metabolites asymmetrically in response to environmental gradients. Importantly, these gradients were formed by plant roots, which may use exudates to shape their microbiomes.[24] Beyond this, our results indicate that metabolite production (e.g., surfactin production in *B. subtilis*) is heterogeneous across microcolonies grown on uniform surfaces. For surfactin

DOI: 10.1021/acs.analchem.9b03909
Anal. Chem. XXXX, XXX, XXX−XXX

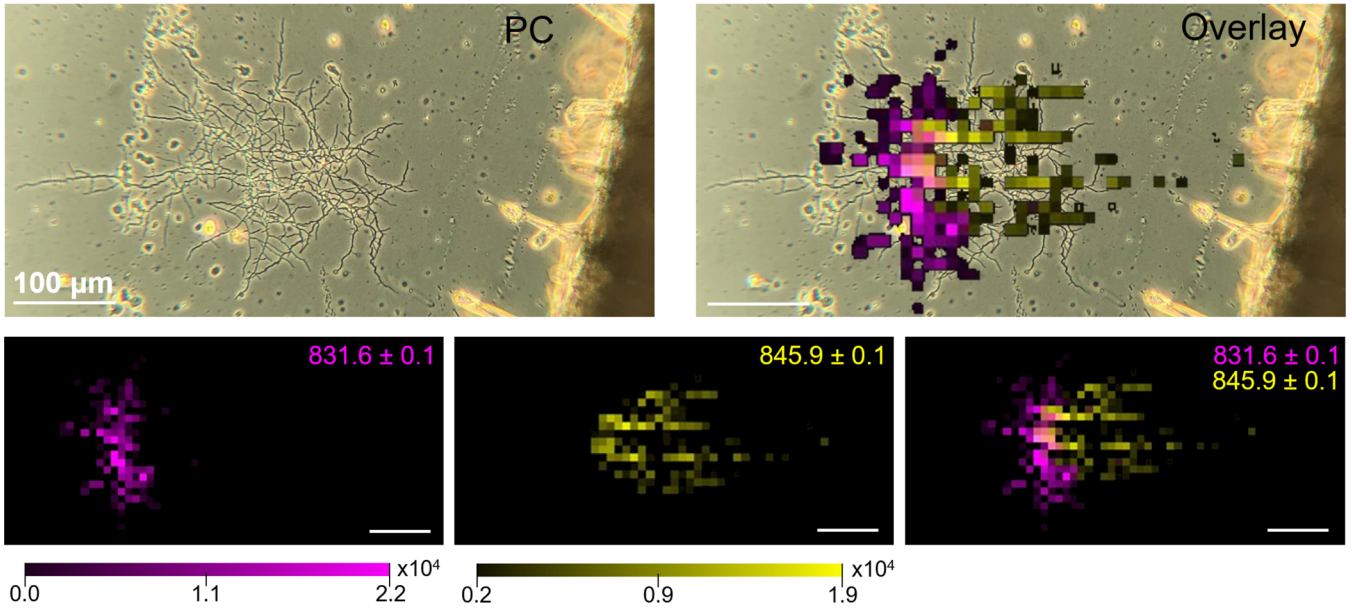

Figure 4. *S. coelicolor* microcolonies display asymmetrical ion distribution when grown in proximity to *Medicago sativa* roots. Micrograph of a *S. coelicolor* microcolony growing near a *M. sativa* root; MALDI images show the spatial distribution of two of the detected features: m/z 831.6 ± 0.1 (a putative uncharacterized lipid) and m/z 845.9 ± 0.1 (an uncharacterized compound). Note the differential localization of the two features within the microcolony. Micrograph was acquired using a phase contrast (PC) microscope.

production, this heterogeneity is likely driven by stochasticity in the regulatory networks that respond to cell−cell signaling.[25,26] Within larger colonies of *S. coelicolor* like those shown in Figure 2, we speculate that metabolite distributions may be driven by changes in the local nutrient environment brought about by microbial growth.

The advances we report here lay the foundation for interrogating the chemical topologies produced by bacteria within diverse microbiomes. Combining this methodology with other imaging techniques that reveal microbial identity (e.g., fluorescent *in situ* hybridization) or gene expression (e.g., fluorescent protein promoter fusions) will provide a multidimensional view of microbial life *in situ* at microscopic scales.

■ ASSOCIATED CONTENT

Supporting Information

The Supporting Information is available free of charge on the ACS Publications website at DOI: 10.1021/acs.analchem.9b03909.

Strains and growth conditions, micrograph acquisition, detailed parameters for all mass spectrometry analyses, and compound identification; Figures S1−S3, MS1 spectra, MALDI images, and MS2 spectra of surfactins and *B. subtilis* lipids; Figures S4−S6, MS1 spectra, MALDI images, and MS2 spectra of *S. coelicolor* lipids; Figure S7, MS1 spectra of the full m/z range of the zoomed in spectra presented in Figures 1B and 2B; Figure S8, TIC of the MALDI-IMS experiments; Figures S9−S11, EIC of m/z range of 745.49−745.50, 1036.68−1036.70, and 831.68−831.70; and Tables S1 and S2, identifications of features of interest (PDF)

■ AUTHOR INFORMATION

Corresponding Author

*E-mail: mtrax@berkeley.edu.

ORCID

Rita de Cassia Pessotti: 0000-0003-0805-8613
Bridget L. Hansen: 0000-0001-5507-7169
Matthew F. Traxler: 0000-0001-8430-595X

Author Contributions

The manuscript was written through contributions of all authors. All authors have given approval to the final version of the manuscript. R.C.P. designed experiments, conducted experiments, analyzed the data, and wrote the paper. M.F.T. designed experiments and wrote the paper. B.L.H. conducted experiments, analyzed the data, and wrote the paper. V.M.Z. analyzed the data and wrote the paper. D.P. conducted experiments.

Notes

The authors declare no competing financial interest.

An early draft of this paper was deposited by us at the recognized preprint server, bioRxiv, before submission to *Analytical Chemistry*. The link to this preprint is https://www.biorxiv.org/content/10.1101/717066v1.

■ ACKNOWLEDGMENTS

This research was supported by PAPM-EAGER Grant 1650059 from the National Science Foundation to M.F.T. and startup funds from University of California, Berkeley to M.F.T.

■ REFERENCES

(1) Drescher, K.; Nadell, C. D.; Stone, H. A.; Wingreen, N. S.; Bassler, B. L. *Curr. Biol.* **2014**, *24* (1), 50−55.
(2) Ghoul, M.; Mitri, S. *Trends Microbiol.* **2016**, *24* (10), 833−845.
(3) Ratzke, C.; Gore, J. *PLoS Biol.* **2018**, *16* (3), No. e2004248.
(4) Abrudan, M. I.; Smakman, F.; Grimbergen, A. J.; Westhoff, S.; Miller, E. L.; van Wezel, G. P.; Rozen, D. E. *Proc. Natl. Acad. Sci. U. S. A.* **2015**, *112* (35), 11054−9.
(5) Cornforth, D. M.; Foster, K. R. *Nat. Rev. Microbiol.* **2013**, *11* (4), 285−93.

DOI: 10.1021/acs.analchem.9b03909
Anal. Chem. XXXX, XXX, XXX−XXX

(6) Vences-Guzman, M. A.; Guan, Z.; Ormeno-Orrillo, E.; Gonzalez-Silva, N.; Lopez-Lara, I. M.; Martinez-Romero, E.; Geiger, O.; Sohlenkamp, C. *Mol. Microbiol.* **2011**, *79* (6), 1496−514.
(7) Sandoval-Calderon, M.; Nguyen, D. D.; Kapono, C. A.; Herron, P.; Dorrestein, P. C.; Sohlenkamp, C. *Front. Microbiol.* **2015**, *6*, 1465.
(8) Rajagopal, M.; Walker, S. *Curr. Top. Microbiol. Immunol.* **2015**, *404*, 1−44.
(9) Ho, Y. N.; Shu, L. J.; Yang, Y. L. *Wiley Interdiscip Rev. Syst. Biol. Med.* **2017**, *9* (5), e1387.
(10) Shih, C. J.; Chen, P. Y.; Liaw, C. C.; Lai, Y. M.; Yang, Y. L. *Nat. Prod. Rep.* **2014**, *31* (6), 739−55.
(11) Yang, J. Y.; Phelan, V. V.; Simkovsky, R.; Watrous, J. D.; Trial, R. M.; Fleming, T. C.; Wenter, R.; Moore, B. S.; Golden, S. S.; Pogliano, K.; Dorrestein, P. C. *J. Bacteriol.* **2012**, *194* (22), 6023−8.
(12) Hankin, J. A.; Barkley, R. M.; Murphy, R. C. *J. Am. Soc. Mass Spectrom.* **2007**, *18* (9), 1646−52.
(13) Kelly, R. T.; Tolmachev, A. V.; Page, J. S.; Tang, K. Q.; Smith, R. D. *Mass Spectrom. Rev.* **2010**, *29* (2), 294−312.
(14) Klinkert, I.; Chughtai, K.; Ellis, S. R.; Heeren, R. M. A. *Int. J. Mass Spectrom.* **2014**, *362*, 40−47.
(15) Bokhart, M. T.; Nazari, M.; Garrard, K. P.; Muddiman, D. C. *J. Am. Soc. Mass Spectrom.* **2018**, *29* (1), 8−16.
(16) Schneider, C. A.; Rasband, W. S.; Eliceiri, K. W. *Nat. Methods* **2012**, *9* (7), 671−5.
(17) Schymanski, E. L.; Jeon, J.; Gulde, R.; Fenner, K.; Ruff, M.; Singer, H. P.; Hollender, J. *Environ. Sci. Technol.* **2014**, *48* (4), 2097−8.
(18) Weart, R. B.; Lee, A. H.; Chien, A. C.; Haeusser, D. P.; Hill, N. S.; Levin, P. A. *Cell* **2007**, *130* (2), 335−47.
(19) Lamb, D. C.; Lei, L.; Zhao, B.; Yuan, H.; Jackson, C. J.; Warrilow, A. G.; Skaug, T.; Dyson, P. J.; Dawson, E. S.; Kelly, S. L.; Hachey, D. L.; Waterman, M. R. *Appl. Environ. Microbiol.* **2010**, *76* (6), 1975−80.
(20) Bais, H. P.; Fall, R.; Vivanco, J. M. *Plant Physiol.* **2004**, *134* (1), 307−19.
(21) Vlamakis, H.; Chai, Y.; Beauregard, P.; Losick, R.; Kolter, R. *Nat. Rev. Microbiol.* **2013**, *11* (3), 157−68.
(22) Debois, D.; Fernandez, O.; Franzil, L.; Jourdan, E.; de Brogniez, A.; Willems, L.; Clement, C.; Dorey, S.; De Pauw, E.; Ongena, M. *Environ. Microbiol. Rep.* **2015**, *7* (3), 570−82.
(23) Debois, D.; Jourdan, E.; Smargiasso, N.; Thonart, P.; De Pauw, E.; Ongena, M. *Anal. Chem.* **2014**, *86* (9), 4431−8.
(24) Sasse, J.; Martinoia, E.; Northen, T. *Trends Plant Sci.* **2018**, *23* (1), 25−41.
(25) Dubnau, D.; Losick, R. *Mol. Microbiol.* **2006**, *61* (3), 564−72.
(26) Lopez, D.; Vlamakis, H.; Losick, R.; Kolter, R. *Genes Dev.* **2009**, *23* (14), 1631−8.

DOI: 10.1021/acs.analchem.9b03909
Anal. Chem. XXXX, XXX, XXX−XXX